

Oumbe A., Wald L., 2010. A parameterisation of vertical profile of solar irradiance for correcting solar fluxes for changes in terrain elevation. In Proceedings of the Earth Observation and Water Cycle Science Conference, 18-20 November, Frascati, Italy. Co-organized by ESA, EGU, ISPRS and GEWEX.

A PARAMETERISATION OF VERTICAL PROFILE OF SOLAR IRRADIANCE FOR CORRECTING SOLAR FLUXES FOR CHANGES IN TERRAIN ELEVATION

Armel Oumbe⁽¹⁾, Lucien Wald⁽²⁾

⁽¹⁾MINES ParisTech - Center for Energy and Processes, BP 207, 06904 Sophia Antipolis, France, Email: armel.oumbe@mines-paristech.fr

⁽²⁾MINES ParisTech - Center for Energy and Processes, BP 207, 06904 Sophia Antipolis, France, Email: lucien.wald@mines-paristech.fr

ABSTRACT

This paper deals with the modelling of vertical profile of solar irradiance for correcting solar radiation data. An approximation of the influence of the terrain elevation on all-skies radiation and a parameterisation of vertical profile on clear-skies radiation are proposed. This parameterisation, called double-z fitting function, is validated using two radiative transfer models. The main applications of this work are: computing clear-sky irradiances from satellite images, extrapolation of irradiances from one site to another of different altitude and correction of databases derived from satellite images.

1. NOMENCLATURE

z, z_0, z_H	altitude (km). Altitude is defined above mean sea level
z_1, z_2	mean sea level
I_0	irradiance at the top of the atmosphere (W m^{-2})
$I(z), B(z)$	global, direct irradiance at altitude z on horizontal plane (W m^{-2})
$I_c(z), B_c(z)$	global, direct irradiance at altitude z on horizontal plane under clear sky (W m^{-2})
f_I, f_B	vertical profile irradiance fitting functions for global, direct irradiance
$A(z), A_B(z)$	attenuation coefficients of the atmosphere for global, direct irradiance (unitless)
α, α_B	parameters of the double-z fitting function (km^{-1})
K_c	clear-sky index. It is equal to the ratio of I to I_c (unitless)
vis	visibility at ground level (km)

2. INTRODUCTION

The surface solar irradiance (SSI) - also called downwelling shortwave irradiance - is an important

element of the surface radiation budget. It is seldom measured and several works have developed methods for the assessment of the surface solar irradiance from images taken by geostationary or polar-orbiting satellites [1, 2]. The various Heliosat methods [3 - 10], the methods of Mueller et al. [11], Perez et al. [12], Raschke et al. [13] or Stuhlmann et al. [14] are based on the principle that the irradiance at a given pixel can be computed by reducing the irradiance that should be observed under clear-sky at that pixel by a certain amount that is a function of the properties of the clouds. Such satellite-derived irradiance data is currently used in various domains, ranging from climate to materials weathering [15].

The computation of the SSI from satellite images calls upon a digital terrain model (DTM) whose cell size fits that of the pixel. For example, the ESRA atlas [16] or the HelioClim-1 database [8] exploits the DTM TerrainBase [17] whose cell size is $5'$ of arc angle, i.e. approximately 10 km at mid-latitude. The size of the cell is even larger for the NASA-SSE database: 1° of arc angle [18] or for the ISIS database: 280 km [19]. Generally, these sizes are too large to describe changes in altitude with a sufficient accuracy in areas of steep relief; large discrepancies can be found between the mean altitude of a cell and the altitude of a particular site within this cell. For example, in Switzerland, the altitude of the measuring station at Saentis Mountain is 2490 m while that provided by the DTM TerrainBase is 1126 m, i.e. an underestimation of 1364 m. If uncorrected, this difference leads to an error in the irradiance provided by the ESRA and HelioClim databases. Note that in very steep relief, irradiance depends upon shadows cast on the sites by surrounding obstacles and not only on change in altitude; this is not the subject of this paper.

Wahab et al. [20] established, for monthly irradiation, that when the difference in altitude reached 200 m, the error on estimated irradiation is significant and conclude that the correction for altitude should be applied in a systematic way. The main objective of this paper is to propose a parameterisation of the vertical variation of SSI with altitude z . Most models for SSI under clear-sky take into account change in SSI with z , whether they are in analytical form [16, 21, 22] or in numerical form such as libRadtran, LOWTRAN or MODTRAN. Laue [23] performed measurements of solar spectral irradiance at different altitudes. Blumthaler et al. [24], Dvorkin and Steinberger [25] focused their work on the UV part of the radiation. Hofierka and Suri [26] propose an empirical relationship between the Linke turbidity factor and the altitude; the corrected factor may then be used in a clear-sky model such as ESRA. No model describing in an explicit manner how the total irradiance changes with z in clear- or all-skies was found in the literature. For practical reasons, it would be convenient to have a simple parameterisation, preferably in analytical form. This would allow e.g., easy implementation in spreadsheet or fast calculation for demonstration and education purposes. It would help in benefiting of the availability of DTM at high spatial resolution such as SRTM: 30 or 90 m [27] to increase the accuracy of the assessment of SSI at a given site. Other applications are possible and three of them are discussed hereafter.

This paper proposes a parameterisation of the vertical profile of the global and direct irradiances. We firstly establish that, in first order, the influence of elevation on SSI in all-skies is equivalent to that in clear-skies. This parameterisation requires solar irradiance at two different altitudes as inputs that can be provided by codes simulating the radiative transfer in atmosphere (RTM: radiative transfer model) or other means. The parameterisation is validated by the results produced by the two RTM: libRadtran and 6S. These RTM are well known and serve as references. The RTM libRadtran was originally developed for modelling UV irradiance [28, 29]. Its accuracy has also been demonstrated for actinic fluxes [30, 31] and total irradiance [11, 19, 32]. The RTM 6S is largely used in processing and simulation of satellites images [33, 34]. Contrary to libRadtran, 6S deals only with clear-sky case.

3. APPROXIMATION OF INFLUENCE OF TERRAIN ELEVATION ON ALL-SKIES

The main factors influencing the SSI under clear-sky $I_c(z)$ received at an altitude z are the ground albedo and optical path. The optical path is mainly influenced by clouds, aerosols and water vapour. Note that this paper deals with total irradiance, i.e., the irradiance received for all wavelengths less than 4 μm . The adjective total is omitted in the following. The ground albedo has an impact on the diffuse component of the irradiance; the greater the albedo, the greater the diffuse component. This impact decreases as the altitude z increases. The optical path is a function of the altitude. As the altitude increases, the thickness of the part of the atmosphere under concern decreases, the optical path decreases leading to a decrease in the attenuation of the radiation, and the downwelling irradiance increases. Besides the purely geometrical effect induced by the reduction of the geometrical path length, the increase in irradiance with z is due to the fact that atmospheric components influencing the radiation under clear skies - water vapour, aerosols - are mostly located in the lower parts of the atmosphere [37].

On many occasions, one wants to know the SSI $I(Q)$ at a site Q of altitude $z(Q)$ but has only observations of SSI $I(P)$ at a site P of altitude $z(P)$. Practically, this is the case of a measuring site on a mountain side (P) and a site of interest located in the valley (Q) or reciprocally. This can be extended to the case where $I(P)$ results from spatial interpolation of neighbouring measuring sites of similar altitude. In this application, the possible exploitation of the fitting functions to all-skies case is discussed. The optical state of the atmosphere, including cloud properties, is assumed the same at P and Q . This means that if P and Q were having the same altitude, the SSI I at P and Q would be equal. It is believed that this assumption is better verified for daily or monthly means of irradiance than for shorter periods of integration. If the clear-sky value $I_c(P)$ at P is known, e.g., by a clear-sky model, the clear-sky index K_c is defined as:

$$I(P) = K_c(P) I_c(P) \quad (1)$$

Thus, the change in I due to change in altitude z is given by

$$\partial I / \partial z = K_c \partial I_c / \partial z + I_c \partial K_c / \partial z \quad (2)$$

LibRadtran is exploited with many different atmospheric conditions to compute each term in Eq. 2. Figure 1 exhibits examples of the changes in SSI and K_c as a function of the cloud optical depth (COD) for

various altitudes. These curves are quasi-independent on the solar zenith angle, visibility, precipitable water, and atmospheric profile; the COD is the major influencing factor.

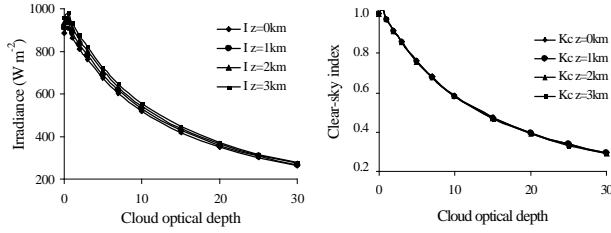


Figure 1. Example of the influence of the cloud optical depth on all-sky irradiance (I) and on clear-sky index (K_c), for different altitudes (z). In these simulations, the water cloud is located between 4 km and 6 km. Clear-sky inputs are solar zenith angle (30°), precipitable water (15 kg m^{-2}), visibility (60 km), number of the day in the year (170), and ground albedo (0.2).

As expected, I and K_c decrease as the COD increases. For a given COD, I increases with the altitude. This is not the case for K_c ; it remains quasi-constant for altitude from 0 km to 3 km. This means that $\partial K_c / \partial z$ is small. The relative contribution of the rightmost term in Eq. 2: $I_c \partial K_c / \partial z$ to $\partial I / \partial z$ is now further investigated. To that purpose, derivatives are written in a discrete form:

$$\partial I / \partial z \approx (I(z_2) - I(z_1)) / (z_2 - z_1) \quad (3)$$

and

$$I_c \partial K_c / \partial z \approx [(I_c(z_2) + I_c(z_1)) / 2] [(K_c(z_2) - K_c(z_1)) / (z_2 - z_1)] \quad (4)$$

where $z_2 = z_1 + 1 \text{ km}$.

Figure 2 displays the comparison between these two terms as a function of the COD.

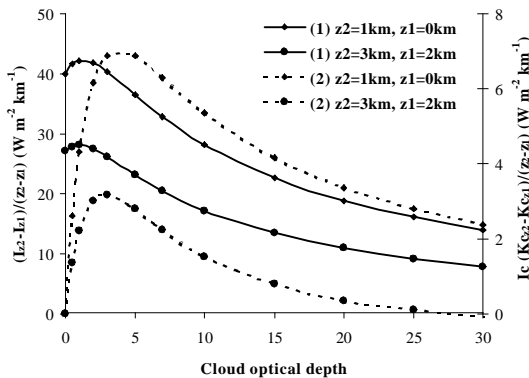


Figure 2. Comparison between $\partial I / \partial z$ (full lines and left axis) and $I_c \partial K_c / \partial z$ (dashed lines, right axis) for different cloud optical depth and altitudes (z). Other inputs are similar to those in figure 1.

$\partial I / \partial z$ reaches its maximum for COD close to 3 and then decreases as the COD increases. $I_c \partial K_c / \partial z$ reaches its maximum for COD between 4 and 6, depending on the altitude. It then decreases as the COD increases. As a whole, the values of $I_c \partial K_c / \partial z$ are approximately 10 times lower than $\partial I / \partial z$. This figure shows that the relative contribution of $I_c \partial K_c / \partial z$ to $\partial I / \partial z$ decreases as the altitude increases and as the COD increases beyond values 4-6. In the studied cases, this relative contribution may reach approximately 20 % but most often is less than 10 %. This means that in most cases, the term $I_c \partial K_c / \partial z$ may be neglected at first order.

Eq. 2 becomes:

$$\partial I / \partial z \approx K_c \partial I_c / \partial z \quad (5)$$

or in a discrete form

$$\frac{[I(Q) - I(P)] / [z(Q) - z(P)]}{[(I_c(Q) - I_c(P)) / (z(Q) - z(P))]} \approx \frac{[(K_c(Q) + K_c(P)) / 2]}{1} \quad (6)$$

or

$$\frac{[I(Q) - I(P)] / [z(Q) - z(P)]}{(I_c(P) [(I_c(Q) - I_c(P)) / (z(Q) - z(P))])} \approx (K_c(P)) \quad (7)$$

It follows:

$$I(Q) - I(P) \approx K_c(P) I_c(Q) - K_c(P) I_c(P) \quad (8)$$

Using Eq. 1 for $I(P)$

$$I(Q) \approx K_c(P) I_c(Q) \quad (9)$$

If an analytical function f_i , describing the vertical profile of the SSI in clear sky I_c

$$I_c(z) = I_c(z_0) f_i(z_0, z, I_c(z_0)) \quad (10)$$

is available, then the irradiance $I(Q)$ at site Q is easily computed as:

$$I(Q) = K_c(P) I_c(P) f_i(z(P), z(Q), I_c(P)) \quad (11)$$

or

$$I(Q) = I(P) f_i(z(P), z(Q), I_c(P)) \quad (12)$$

Thus, the function used to model the vertical profile in clear-sky can be used in all-skies conditions at first order.

4. PARAMETERISATION OF VERTICAL PROFILE IN CLEAR-SKY

As a consequence of the previous conclusion, it follows that the search for a parameterisation of vertical profile of SSI can be restricted to clear-sky case.

Figure 3 shows an example of vertical profiles of global I_c and direct B_c irradiances. Both profiles are superimposed at high altitude where the scattering effects are small and consequently, the diffuse

irradiance is small. Close to sea level ($z = 0$), both profiles differ because of the increasing role of the scattering effects. Most of the photons removed from the direct beam end up as diffuse irradiance. Global irradiance is therefore always larger than direct irradiance. This figure clearly shows that the direct and global components decrease with z . For example, there is a decrease of 30 W m^{-2} in direct irradiance between 1 km and 0.5 km.

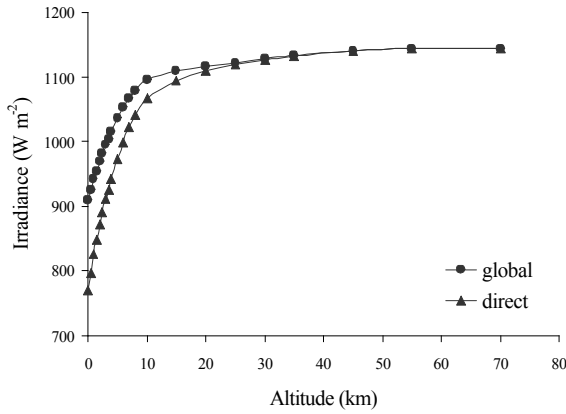


Figure 3. Example of vertical profiles of direct and global irradiances. These profiles have been computed with the radiative transfer model libRadtran. Main input parameters were solar zenith angle (30°), precipitable water (15 kg m^{-2}), visibility (60 km), number of the day in the year (170), and ground albedo (0.2).

We are looking for analytical functions f_I and f_B that model the vertical profile of global $I_c(z)$ and direct $B_c(z)$ irradiances under clear-sky at any altitude z starting from known values of $I_c(z_0)$ and $B_c(z_0)$ at an altitude z_0 :

$$I_c(z) = I_c(z_0) f_I(z_0, z, I_c(z_0)) \quad (13)$$

$$B_c(z) = B_c(z_0) f_B(z_0, z, B_c(z_0))$$

where f_I is the quantity to be determined for the global irradiance I_c , f_B that for the direct component B_c and I_0 the irradiance at the top of the atmosphere. Our work is based on the assumption that within the range of terrain altitude on the earth: 0 to 8 km, the vertical profile of irradiance follows an exponential form. This assumption is supported by the law of Beer-Bouguer-Lambert and by the ESRA model [16]. Fig.3 illustrates the soundness of this assumption. Note that this assumption is more appropriate to the direct irradiance than to the global irradiance.

Knowing two values of clear-sky irradiances $I_c(z_0)$ and $I_c(z_H)$ at two different altitudes z_0 and z_H allows to define the parameters of a fitting function in a deterministic

way. This fitting function is called “double-z fitting function” because it needs as inputs the clear-sky irradiances at two altitudes. Two attenuation coefficients, $A(z)$, for global and, $A_B(z)$, for direct irradiances are defined:

$$I_c(z) = I_0 (1 - A(z)) \quad (14)$$

$$B_c(z) = I_0 (1 - A_B(z))$$

It is assumed that $A(z)$ and $A_B(z)$ have the following forms:

$$A(z) = A(z_0) \exp[-\alpha(z - z_0)] \quad (15)$$

$$A_B(z) = A_B(z_0) \exp[-\alpha_B(z - z_0)]$$

Then $A(z_0)$ and α are determined from Eqs 14 and 15:

$$A(z_0) = 1 - (I_c(z_0) / I_0) \quad (16)$$

$$\alpha = -\ln[(I_0 - I_c(z_H)) / (I_0 - I_c(z_0))] / (z_H - z_0) \quad (17)$$

where z_H has been empirically defined, in km, as:

$$z_H = \max(3, z_0 + 2) \quad (18)$$

after several trials.

The same equations hold for $A_B(z_0)$ and α_B , where $B_c(z_H)$ and $B_c(z_0)$ are the direct clear-sky irradiances at z_H and z_0 :

$$A_B(z_0) = 1 - (B_c(z_0) / I_0) \quad (19)$$

$$\alpha_B = -\ln[(I_0 - B_c(z_H)) / (I_0 - B_c(z_0))] / (z_H - z_0) \quad (20)$$

This parameterisation would allow e.g., easy implementation in spreadsheet or fast calculation for demonstration and education purposes. An alternative to the analytical parameterisation is a method based on look-up tables or abacus. The irradiances $I_c(z)$ and $B_c(z)$ are computed by invoking libRadtran for a large number of cases that are representative of all expected cases. Great attention should be brought to the description of aerosol properties as they are presently not well known and have a crucial importance on the clear sky irradiance [19, 35]. An example of these representative cases can be the following:

- every 1 km in altitude, from 0 km to 9 km,
- every 5° in solar zenith angle, from 0° to 75° ,
- every 10 km in visibility, from 10 km to 110 km,
- four types of aerosol in the lower 2 km of atmosphere: rural, maritime, urban and tropospheric,
- every 10 kg m^{-2} in precipitable water, from 10 kg m^{-2} to 80 kg m^{-2} ,
- six atmosphere profiles: tropical, midlatitude summer, midlatitude winter, subarctic summer, subarctic winter and U.S standard,
- and every 0.2 in ground albedo, from 0 to 0.8.

The results are stored in look-up tables. For any set of inputs, the irradiances are computed by interpolation of

the known values stored in the look-up tables. Such a method would be similarly accurate and fast.

Both solutions have benefits and drawbacks. The analytical parameterisation is easy to handle and to implement. But, observations at two different altitudes of clear-sky irradiances at the same instant and same place are very rare. The look-up tables are cumbersome to compute and then to implement in the routine operations. For efficiency, the look-up tables -whose size would be approximately 200 Mbytes- should be stored in computer memory. The accuracy of the analytical parameterisation cannot be increased, except if the parameterisation is changed. The accuracy in the look-up tables can be improved by decreasing the quantification step in all inputs at the expenses of the increase of the initial computation and of the size of the look-up tables. If new descriptions of aerosol properties are available, the analytical parameterisation adapt itself to changing conditions while the look-up tables should be recomputed for the new conditions and re-implemented in the processing software.

5. COMPARISON WITH TWO RTM

The outcomes of this double-z fitting function are compared for several altitudes to the outcomes of libRadtran which serves here as a reference. LibRadtran was run for several input conditions, e.g., different solar zenith angle (0, 10, 20, 40, 50, 60, 65, 70, 75, 80) deg, four different aerosol types, different visibilities (15, 20, 25, 30, 40, 50, 60, 80, 100) km, different amounts of precipitable water (10, 15, 30, 60, 80) kg m⁻², different standard atmospheres and different ground albedos (0.0, 0.2, 0.3, 0.6, 0.9). Similar runs were made with 6S. Similar conclusions and values were obtained, ensuring that the comparison is not biased by the use of a single RTM.

Fig. 4 illustrates the performance in the form of the relative deviation in percentage, between the vertical profiles (from 0 km to 9 km) obtained by the fitting function and those obtained by libRadtran, in the case where z_0 is set to mean sea level. As a whole, it is observed that the relative deviation is larger for the direct irradiance than for the global irradiance. There is a dependency of the deviation with the altitude with no clear trend. Quite often, the deviation decreases when the visibility increases but not always. The visibility and

solar zenith angle are the most influencing factors on the vertical profile and therefore on the performance of a fitting function to reproduce the profile. The amount of precipitable water has little effect on the deviation.

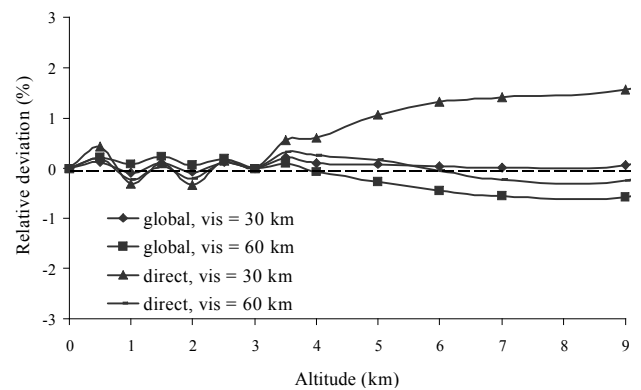


Figure 4. Relative deviation obtained with the double-z fitting function. global (direct) means global (direct) irradiance, vis means “visibility”, and other conditions are those in Fig. 3. z_0 is equal to 0 km.

Fig. 5 shows that there is little influence of the solar zenith angle on the deviation. Deviation is a function of the altitude. The deviation tends to increase when z_0 increases. But it remains very small, between -0.2% and 0.2% for altitudes up to 5 km, for standard atmospheric conditions and a solar zenith angle of 30° .

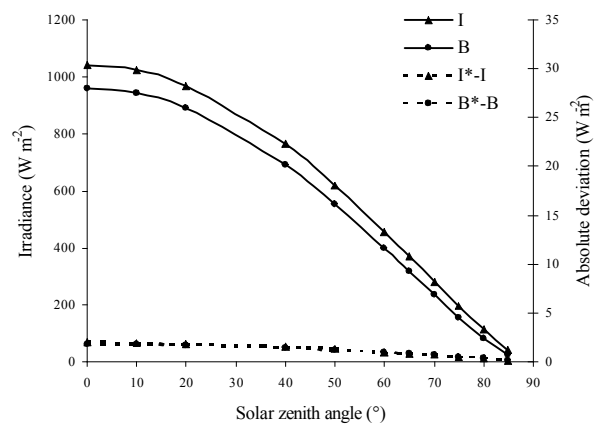


Figure 5. Example of the influence of the solar zenith angle. I and B are estimated from 6S. Irradiances I^* and B^* are assessed at $z = 1$ km with $z_0 = 0$ km (full line, left axis). Also shown are the deviations between respectively I and I^* , and B and B^* (dashed line, right axis). Other conditions are those in Fig. 3

Generally, the relative deviation is less than 1% (global) or 2% (direct) for current visibilities, i.e. greater than 30 km (WMO 1981). It may amount to respectively 3% and 5% for very low visibilities of 15 km. For larger visibilities, the relative deviation is

almost zero for altitudes from sea level up to 6-7 km (Fig. 4). Given current visibilities and solar zenith angles less than 75° , the relative deviations compare favourably to typical deviations on ground measurements, which are 5 % to 7 % [36].

Since in practice, discrepancies on altitude are generally less than 1 km, it is of interest to evaluate the ability to correct the irradiance assessed incorrectly at a given altitude z_0 while the actual altitude is $z = z_0 + 1$ km. Given the irradiance $I_c(z_0)$ and $I_c(z_H)$, the double-z fitting function is applied to compute an estimate $I_c^*(z)$. This estimate is then compared to the correct value $I_c(z)$ given by libRadtran and the difference is computed. This comparison is performed for various atmospheric conditions and various z_0 . Table 1 shows example of the deviations reached by the double-z fitting function for different z_0 . One can see that the double-z fitting function exhibit small relative deviations, often less than 1 %, for global and direct irradiances. It is concluded that this function may be used to correct satellite-derived SSI.

z_0 (km)	Direct irradiance		Global irradiance	
	vis 30	vis 60	vis 30	vis 60
0	-0.6 (-0.1 %)	-1.5 (-0.4 %)	-1.4 (-0.3 %)	-0.2 (-0.1 %)
1	-1.2 (-0.3 %)	-0.8 (0.2 %)	-0.5 (-0.1 %)	0.01 (0.0 %)
2	-2.0 (-0.4 %)	-0.7 (-0.1 %)	-0.7 (-0.1 %)	-0.2 (-0.0 %)
3	-0.7 (-0.1 %)	0.9 (0.2 %)	0.0 (0.0 %)	0.5 (0.1 %)
4	0.2 (0.0 %)	1.1 (0.2 %)	0.3 (0.1 %)	0.6 (0.1 %)
5	0.4 (0.1 %)	0.4 (0.1 %)	0.1 (0.0 %)	0.1 (0.0 %)
6	-0.2 (-0.0 %)	-0.2 (-0.0 %)	-0.1 (-0.0 %)	-0.1 (-0.0 %)
7	-0.5 (-0.1 %)	-0.5 (-0.1 %)	-0.2 (-0.0 %)	-0.2 (-0.0 %)

Table 1. Error (in W m^{-2}) between actual irradiance $I_c(z_0+1)$ provided by libRadtran and the irradiance predicted by fitting functions. The relative deviation is indicated in brackets. Two visibilities are reported: 30 km (vis 30) and 60 km (vis 60). Solar zenith angle is 60° . Other conditions are those in Fig.3.

6. CONCLUSION

This study demonstrates that it is possible to find fitting functions that reproduce the vertical profile of the global

and direct irradiances under clear-sky with sufficient accuracy. The possibility of using look-up-tables for the same purpose is also discussed. It is shown that in first order, the influence of altitude on all-sky irradiance is equivalent to the influence of altitude on the corresponding clear-sky irradiance. It follows that any fitting function developed for clear-sky can be used in all-sky conditions. It is also found that the double-z fitting function might be used to correct irradiance with a sufficient accuracy in the case where irradiance is incorrectly assessed because of a deviation in altitude. This result can be exploited in the case of extrapolating irradiance measuring at a station to a close site of different altitude and also in the case of design a fast method for processing satellite data based on RTM.

REFERENCES

1. Ba, B.M., Frouin, R., Nicholson, S.E., Dedieu G., 2001. Satellite-Derived Surface Radiation Budget over the African Continent. Part I: Estimation of Downward Solar Irradiance and Albedo. *Journal of Climate*, vol. 14 (1), 45-58.
2. Pinker, R.T., Laszlo, I., 1991. Effects of spatial sampling of satellite data on derived surface solar irradiance. *Journal of Atmospheric and Oceanic Technology*, 8, 96-107.
3. Cano, D., Monget, J.-M., Albuissou, M., Guillard, H., Regas, N., Wald, L., 1986. A method for the determination of the global solar radiation from meteorological satellite data. *Solar Energy*, 37 (1), 31-39.
4. Beyer, H.-G., Costanzo, C., Heinemann, D., 1996. Modifications of the Heliosat procedure for irradiance estimates from satellite images. *Solar Energy*, 56 (3), 207-212.
5. Diabaté, L., Demarcq, H., Michaud-Regas, N., Wald, L., 1988. Estimating incident solar radiation at the surface from images of the Earth transmitted by geostationary satellites: the Heliosat Project. *International Journal of Solar Energy*, 5, 261-278.
6. Diabaté, L., Moussu, G., Wald, L., 1989. Description of an operational tool for determining

global solar radiation at ground using geostationary satellite images. *Solar Energy*, 42(3), 201-207.

7. Hammer, A., 2000. Anwendungsspezifische Solarstrahlungsinformationen aus Meteosat-Daten. Dissertation, Carl von Ossietzky Universität Oldenburg, Fachbereich Physik, Oldenburg, Germany.
8. Lefèvre, M., Diabaté, L., Wald, L., 2007. Using reduced data sets ISCCP-B2 from the Meteosat satellites to assess surface solar irradiance. *Solar Energy*, 81 (2), 240-253.
9. Pastre, C., 1981. Développement d'une méthode de détermination du rayonnement solaire global à partir des données Meteosat. La Météorologie, VIe série, N°24.
10. Rigollier, C., Lefèvre, M., Wald, L., 2004. The method Heliosat-2 for deriving shortwave solar radiation from satellite images. *Solar Energy*, 77 (2), 159-169.
11. Mueller, R., Dagestad, K.F., Ineichen, P., Schroedter, M., Cros, S., Dumortier, D., Kuhlemann, R., Olseth, J.A., Piernavieja, G., Reise, C., Wald, L., Heinemann, D., 2004. Rethinking satellite based solar irradiance modelling - The SOLIS clear sky module. *Remote Sensing of Environment*, 91 (2), 160-174.
12. Perez, R., Ineichen, P., Moore, K., Kmiecik, M., Chain, C., George, R., Vignola, F., 2002. A new operational model for satellite-derived irradiances description and validation. *Solar Energy*, 73 (5), 307-317.
13. Raschke, E., Stuhlmann, R., Palz, W., Steemers, T.C., 1991. Solar Radiation Atlas of Africa. A. Balkema, Rotterdam, The Netherlands. p. 155.
14. Stuhlmann, R., Rieland, M., Raschke, E., 1990. An improvement of the IGMK model to derive total and diffuse solar radiation at the surface from satellite data. *Journal of Applied Meteorology*, 29, 596-603.
15. Gschwind, B., Ménard, L., Albuisson, M., Wald, L., 2006. Converting a successful research project into a sustainable service: the case of the SoDa Web service. *Environmental Modelling and Software*, 21 (11), 1555-1561, doi:10.1016/j.envsoft.2006.05.002.
16. ESRA, 2000. European Solar Radiation Atlas, fourth ed., includ. CD-ROM. Edited by Greif, J., and K. Scharmer. Scientific advisors: R. Dogniaux, J. K. Page. Authors: L. Wald, M. Albuisson, G. Czeplak, B. Bourges, R. Aguiar, H. Lund, A. Joukoff, U. Terzenbach, H. G. Beyer, E. P. Borisenko. Published for the Commission of the European Communities by Presses de l'Ecole, Ecole des Mines de Paris, Paris, France.
17. TerrainBase, 1995. Worldwide digital terrain data, Documentation Manual, CD-ROM Release 1.0, April 1995, NOAA, National Geophysical Data Center, Boulder, CO, USA.
18. Chandler, W. S., Whitlock, C. H., Stackhouse, P. W. Jr., 2004. NASA climatological data for renewable energy assessment. *Journal of Solar Energy Engineering*, 126(3), 945-949.
19. Lohmann, S., Schillings, C., Mayer, B., Meyer, R., 2006. Long-term variability of solar direct and global irradiance derived from ISCCP data and comparison with re-analysis data. *Solar Energy*, 80, 1390-1401.
20. Wahab, M., El-Metwally, M., Hassan, R., Lefèvre, M., Oumbe, A., and Wald, L., 2009. Assessing surface solar irradiance in northern africa desert climate and its long-term variations from meteosat images. *International Journal of Remote Sensing*, in press.
21. Iqbal, M., 1983. *An Introduction to Solar Radiation*. Academic Press, New York, USA, 373 p.
22. Gueymard, C., 1995. SMARTS2, A simple model of the atmospheric radiative transfer of sunshine: algorithms and performance assessment, FSEC-PF-270-95. Professional Paper, Florida Solar Energy Center, 84 p.
23. Laue, E.G., 1970. The measurement of solar spectral irradiance at different terrestrial altitudes. *Solar Energy*, 13 (1), 43-47.

24. Blumthaler, M., Ambach, W., Ellinger, R., 1997. Increase in solar UV radiation with altitude. *Journal of Photochemistry and Photobiology B: Biology*, 39 (2), 130-134.
25. Dvorkin, A. Y., Steinberger, E. H., 1999. Modelling the altitude effect on solar UV radiation. *Solar Energy*, 65 (3), 181-187.
26. Hofierka, J., Suri, M., 2002. The solar radiation model for Open source GIS: implementation and applications. In Proceedings of the Open source GIS - GRASS users conference 2002 - Trento, Italy, pp. 1-19.
27. Van Zyl, J., 2001. The Shuttle Radar Topography Mission (SRTM): a breakthrough in remote sensing of topography. *Acta Astronautica*, 48, Issues 5-12, 559-565.
28. Bernhard, G., Booth, C. R., Ebrahimian, J. C., 2002. Comparison of measured and modeled spectral ultraviolet irradiance at Antarctic stations used to determine biases in total ozone data from various sources. In Ultraviolet Ground-and Space-based Measurements, Models, and Effects, edited by J.R. Slusser, J.R. Herman, and W. Gao, Proceedings of SPIE, Vol. 4482, 115-126.
29. Balis, D. S., Amiridis, V., Zerefos, C., Kazantzidis, A., Kazadzis, S., Bais, A. F., Meleti, C., Gerasopoulos, E., Papayannis, A., Matthias, V., Dier, H., Andreae, M. O., 2004. Study of the effect of different type of aerosols on UV-B radiation from measurements during EARLINET. *Atmospheric Chemistry and Physics* 4, 307-321.
30. Kylling, A., Webb, A. R., Kift, R., Gobbi, G. P., Ammannato, L., Barnaba, F., Bais, A., Kazadzis, S., Wendisch, M., Jakel, E., Schmidt, S., Kniffka, A., Thiel, S., Junkermann, W., Blumthaler, M., Silbernagl, R., Schallhart, B., Schmitt, R., Kjeldstad, B., Thorseth, T. M., Scheirer, R., Mayer, B., 2005. Spectral actinic flux in the lower troposphere: measurement and 1-D simulations for cloudless, broken cloud and overcast situations. *Atmospheric Chemistry and Physics*, 5, 1975-1997.
31. Thiel, S., Ammannato, L., Bais, A., Bandy, B., Blumthaler, M., Bohn, B., Engelsen, O., Gobbi, G. P., Grobner, J., Jakel, E., Junkermann, W., Kazadzis, S., Kift, R., Kjeldstad, B., Kouremeti, N., Kylling, A., Mayer, B., Monks, P. S., Reeves, C. E., Schallhart, B., Scheirer, R., Schmidt, S., Schmitt, R., Schreder, J., Silbernagl, R., Topaloglou, C., Thorseth, T. M., Webb, A. R., Wendisch, M., Werle, P., 2007. Influence of clouds on the spectral actinic flux density in the lower troposphere (INSPECTRO): overview of the field campaigns. *Atmospheric Chemistry and Physics Discussions*, 7, 13417-13473.
32. Ineichen, P., 2006. Comparison of eight clear sky broadband models against 16 independent data banks. *Solar Energy*, 80 (4), 468-478.
33. Vermote, E., Tanré, D., Deuzé, J. L., Herman, M., Morcrette, J. J., 1997. Second simulation of the satellite signal in the solar spectrum (6S), 6S: An overview. *IEEE Transactions on Geoscience and Remote Sensing*, 35, 675-686.
34. Gascon, F., Gastellu-Etchegorry, J.-P., Lefèvre, M.-J., 2001. Radiative transfer model for simulating high-resolution satellite images. *IEEE Transactions on Geoscience and Remote Sensing*, 39 (9), 1922-1926.
35. Breitzkreuz, H., Schroedter-Homscheidt, M., Holzer-Popp, T., 2007. A case study to prepare for the utilization of aerosol forecasts in solar energy industries. *Solar Energy*, 81(11), 1377-1385.
36. World Meteorological Organization (WMO), 1981. Meteorological aspects of the utilization of solar radiation as an energy source. Annex: World maps of relative global radiation. Technical Note N° 172, WMO-N° 557, Geneva, Switzerland, 298 pp.
37. Liou K.N., 1980, *An Introduction to Atmospheric Radiation*. International Geophysics Series, volume 26, Academic Press, 392 p.